Effect of Pushover Load Pattern on Seismic Responses of RC Frame Buildings

Mohammed H. Serror[1], Nayer A. El-Esnawy[2], and Rania F. Abo-Dagher[3]

[1] Assistant Professor, Dept. of Structural Engineering, Faculty of Engineering, Cairo University, Egypt
[2] Professor, Dept. of Structural Engineering, Faculty of Engineering, Cairo University, Egypt
[3] M.Sc. Graduate, Dept. of Structural Engineering, Faculty of Engineering, Cairo University, Egypt
mhassanien@cosmos-eng.com

Abstract: Recently, attention has been paid to the performance-based seismic design that requires designing the building for several expected performance levels. This is achievable through a design procedure based on the inelastic responses. In order to estimate the inelastic seismic responses of a building, the pushover analysis is used, for its simplicity compared with the nonlinear time-history analysis. In pushover analysis, however, the first step is to select a particular lateral load pattern, which affects the resulting capacity curve that may over- or under-estimate building seismic capacity. Therefore, the selection of a reasonable lateral load pattern is particularly important in pushover analysis. The aim of this study is to analyze the effect of lateral load patterns on the seismic performance of low-to-mid-rise Reinforced Concrete (RC) frame buildings. The RC frame buildings, which consist of 6, 9, and 12 stories, are designed according to Egyptian codes ECP-201 and ECP-203. The lateral load patterns for pushover analysis are selected as uniform, inverted triangle, first mode, IBC (k=2), and weighted-load vector patterns. Pushover analysis has been performed according to FEMA-356 guidelines. The effect of the selected lateral load patterns on the seismic responses of the RC frame buildings is illustrated. In particular, the top drift of the building, the base shear, and the peak inter-story drift are analyzed.

1. Introduction

The current codes for seismic design have the objectives to assure life safety (strength and ductility) and damage control (serviceability limits). The design criteria, accordingly, are formulated based on limits on stresses and member forces calculated from prescribed levels of applied lateral force. The performance-based design, however, is a more general design philosophy in which the design criteria are expressed in terms of achieving stated performance objectives when the structure is subjected to stated levels of seismic hazard (**Ghobarah, 2001**).

SEAOC Vision 2000 **(1995)** has developed a framework that is able to accommodate multiple performance objectives; meanwhile, it addresses the performance levels for structural and non-structural systems. The Applied Technology Council (**ATC 40, 1996**) has developed a procedure that involves determining the capacity and demand spectra. At the performance point, the seismic capacity is assumed equal to the demand, which provides an estimate of acceleration (strength) and displacement (demand). The Federal Emergency Management Agency (**FEMA 273, 1997**) has defined performance levels for structural systems, and proposed drift limits for various lateral-load resisting systems at different performance levels. Moreover, it addresses concepts, philosophy, design methodologies and various applications of performance-based design.

It is worth noting that demand evaluation at the low performance levels requires the consideration of the inelastic behavior of the building. Although seismic demands can be determined by inelastic dynamic analysis using the acceleration time-history of a given earthquake, the engineers prefer simple and less expensive procedures for every day design. Accordingly, the pushover analysis has been proposed by recent seismic design codes. Pushover methods have been a practical tool for building evaluation considering the performance-based engineering in several international seismic codes such as the **FEMA 273 (1997)**, Euro-code 8 (EC-8), and International Building Code (**IBC-2003**). In these seismic regulations, pushover methods such as N2- method, Capacity Spectrum method, and Displacement coefficient method are recommended for determining the inelastic responses of the building during earthquake events.

In the pushover analysis, the first step is to select a particular lateral load pattern, which affects the resulting capacity curve that may over- or under-estimate building seismic capacity. **Akbas *et al.* (2003)** reported the change in failure mode under

increasing shear force distribution in the inelastic region. It was reported also that a triangular load distribution underestimate the base shear compared to the uniform load distribution. **Jianguo *et al.* (2006)** studied pushover analysis of 10-story moment resisting frame (MRF) composed of concrete filled rectangular tubular (CFRT) columns, reinforced concrete columns and steel beams. They concluded that pushover analysis results are sensitive to lateral load patterns and it was recommended to use at least two load patterns to properly estimate the internal forces. **Korkmaz *et al.* (2003)** evaluated the performance of frame structures for three lateral load patterns and four natural periods by performing pushover and nonlinear dynamic time history analyses. They concluded that pushover analysis results do not match with the nonlinear dynamic time history analysis results for any frame structures; meanwhile, the rectangular load pattern estimates maximum and more reasonable seismic demands than triangular and IBC (*k*=2) load patterns. **Intel *et al.* (2003)** evaluated the accuracy of various lateral load patterns used in pushover analysis procedures. First mode, triangular, rectangular, IBC, and multimode patterns were applied on four buildings consisting of 3- and 9-story regular steel moment resisting frames. Nonlinear dynamic time history analysis has been performed using eleven ground motion records. They concluded that estimates of inter-story drift, story shear and overturning moment were generally improved when multiple modes were considered. Meanwhile, the pushover results indicated that first mode lateral load pattern can be made without an appreciable loss of accuracy. Therefore, the selection of a reasonable lateral load pattern is particularly important in pushover analysis.

The aim of this study is to analyze the accuracy of different pushover load patterns. The effect of higher modes is beyond the scope of this paper. Hence, seismic evaluation has been performed for low- to medium-rise RC frames. The study has interfaced the four performance levels of FEMA 273 as shown in Fig. 1a. The performance levels, from high-to-low, are: immediate occupancy (IO, drift<0.2%), operational (drift <0.5%), life safety (LS, drift<1.5%), and collapse prevention (CP, drift<2.5%). Relevant to these performance levels, plastic hinge behavior (force-displacement/ moment-rotation) has been defined in relation to the performance curve as shown in Fig. 1b. The plastic hinge formation has been incorporated in the pushover analysis.

2. Description of Building Models

Fig. 2 shows the typical floor plan and building elevation of the models that have been considered in this study. The buildings are assumed to be of residential function in the great Cairo region with symmetrical system described by reinforced concrete (RC) moment-resisting frames. For the selected buildings, the typical bay width is 5.0m and the typical floor height is 3.0m, except for the first floor height which is considered to be 4.0m. All columns are assumed to be fixed at the foundation level. It is worth noting that two-dimensional analysis has been performed for two intermediate moment-resisting frames along one of the horizontal directions, namely: frame Case-A, and frame Case-B as shown in Fig. 2a. Based on pilot analyses, it has been observed that no significant difference exists between Case-A and Case-B; accordingly, analysis results for only Case-A has been reported in this study.

For a typical three-bay RC moment-resisting frame, different heights are considered: 6, 9, and 12 stories. The frames are designed in accordance with the Egyptian code for design and construction of RC structures (**ECP-203, 2007**). The concrete properties have been selected to have a characteristic compressive strength of 25N/mm2, a specific weight of 25KN/m3, an elastic modulus of 22KN/mm2, and Poisson's ratio of 0.2. Meanwhile, the reinforcement rebars are selected to have a yielding strength of 360N/mm2, an elastic modulus of 210KN/mm2, and Poisson's ratio of 0.3. The design loads, on the other hand, are determined in accordance with the Egyptian code for loads and forces (**ECP-201, 1993**). The dead load including own weight, flooring, and partitions is assumed to be 7.0KN/m2. Meanwhile, the live load is assumed, within the specified range of the Egyptian code, to be 2.5 KN/m2. Table 1 shows the dimensions and reinforcement of the 6-, 9-, and 12-story buildings.

SAP2000 program (**CSI, 2010**) has been used for the pushover analysis of building models. The program has the capability to model the plastic hinge behaviour at prescribed discrete points that are placed at beam and column ends. The plastic hinge properties have been characterized in accordance with **FEMA-356 (2000)** criteria. The plastic hinge deformation curve declares the nonlinear relationship between force and displacement (moment and rotation) at the plastic hinge location as shown in Fig. 1b. This figure gives the yield value and plastic deformation in terms of five points, A-B-C-D-E. Point-A represents the origin, Point-B represents the yielding state, Point-C represents the ultimate capacity of the plastic hinge, Point-D represents the residual strength of the plastic hinge, and Point-E represents the total failure of the plastic hinge. It is worth noting that no deformation occurs in the plastic

hinge up to Point-B; in addition, the displacement (rotation) at Point-B will be subtracted from the values at C, D, and E. Hence, the plastic deformation beyond Point-B will be exhibited by the plastic hinge. Beyond Point-E the hinge will drop load down to zero.

3. Pushover load patterns

Six lateral load patterns have been considered in this study, namely: uniform, inverted triangle, first mode, IBC, and weighted-load vector WLVP1 and WLVP2. The uniform load pattern (UNF) is recommended by FEMA-356 (2000) for the pushover analysis of buildings. For this pattern, the load at the ith floor (P_i) is proportional to the ith floor mass (m_i) and is defined by:

$$P_i \, \alpha \, m_i \qquad (1)$$

The inverted triangular load pattern (TRG) is considered equivalent to the first mode shape of building vibration, where the mode shape varies linearly over building height. For this pattern, the load at the ith floor (P_i) is proportional the ith floor mass (m_i) and height from the foundation (h_i) and is defined by:

$$P_i \, \alpha \, m_i h_i \qquad (2)$$

The first mode load pattern (MOD1) is related to the first mode shape of vibration $\{\phi\}$ by:

$$P \, \alpha \, M\{\phi\} \qquad (3)$$

Where P is the lateral force vector and M is the mass matrix of the equivalent Multi-Degree-of-Freedom (MDOF) system. Hence, the lateral load at the ith floor is proportional to the ith component of the first mode shape $\{\phi_i\}$ and the floor mass (m_i) and is defined by:

$$P_i \, \alpha \, m_i\{\phi_i\} \qquad (4)$$

The lateral load patterns can be determined by the international building code (IBC) as follows:

$$P_i = V \cdot \left(w_i h_i^k \bigg/ \sum_{j=1}^{n} w_j h_j^k \right) \qquad (5)$$

Where V is the design base shear, w_i and wj are the portion of the total gravity load of the structure located at the level i or j, h_i and hj are the height from the base to the level i or j, and k is an exponent related to the effective fundamental period of the structure. In this study, the k factor has been considered equal to 2.

The weighted load-vector pushover method

(**El-Esnawy, 2007**) is based on a lateral load pattern that combines the peak equivalent static forces of the first two modes of vibration. These patterns are determined as follows:

$$\{f_{wv1}\} = \{f_1\} + \{f_2\} \qquad (6)$$

$$\{f_{wv2}\} = \{f_1\} - \{f_2\} \qquad (7)$$

$$\{f_1\} = \Gamma_1 \cdot S_{a,1} [M] \cdot \{\Phi_1\} \cdot \Psi_1 \qquad (8)$$

$$\{f_2\} = \Gamma_2 \cdot S_{a,2} \cdot [M] \cdot \{\Phi_2\} \cdot \Psi_2 \qquad (9)$$

$$[M] \cdot \{\Phi_1\} = \{m_1\Phi_{1,1} \quad m_2\Phi_{2,1} \quad m_3\Phi_{3,1} \quad . \quad . \quad m_N\Phi_{N1}\}^T \qquad (10)$$

$$[M] \cdot \{\Phi_2\} = \{m_1\Phi_{1,2} \quad m_2\Phi_{2,2} \quad m_3\Phi_{3,2} \quad . \quad . \quad m_N\Phi_{N2}\}^T \qquad (11)$$

Where $\{f_{wv1}\}$ is the first weighted-vector lateral load pattern (WVLP1), $\{f_{wv2}\}$ is the second weighted-vector lateral load pattern (WVLP2), Γ_1 and Γ_2 are the first and the second modal participation factors, respectively, $S_{a,1}$ and $S_{a,2}$ are the elastic spectral acceleration corresponding to the first and the second periods of vibration T_1 and T_2, respectively, using Type (I) response spectrum of **ECP-201 (2007)**, Ψ_1 and Ψ_2 are the first and the second effective modal mass ratios, respectively, m_N is the mass of the Nth floor, $\Phi_{N,1}$ is the deformed shape corresponding to mode-1, $\Phi_{N,2}$ is the deformed shape corresponding to mode-2. A more general modal procedure for consideration of higher modes contribution is addressed by **Chopra and Goel (2002)** and known as modal pushover analysis (MPA).

The abovementioned lateral load patterns have been normalized to the uniform load pattern. Hence, pushover analysis has been performed for each RC model under a set of six lateral load patterns. SAP2000 program has been used in the analysis and the plastic hinge properties of FEMA 356 have been interfaced. For each model and, in turn, for each lateral load pattern, the capacity curve has been developed and a set of seismic responses have been investigated, namely: base shear ratio to the building weight, ductility reduction factor, and inter-story drift ratio. Moreover, the seismic responses have been analyzed. Hereafter, analysis results have been presented and discussed.

4. Results and Discussion

Figs. 3a-3c show the capacity curves for the 6-, 9- and 12-story models, respectively. The base shear (V) is normalized to the building weight (W); similarly, the lateral drift (D) is normalized to the building height (H). It is obvious that the capacity curve is affected by the choice of pushover load

pattern which, in turn, may over- or under-estimate the building seismic capacity. The characteristics of the resulted capacity curves may be summarized as follows: (1) the UNF pattern represents an upper bound for seismic capacity, (2) the WVLP2 and IBC patterns represent a lower bound for seismic capacity, (3) the WVLP1 pattern represents an average for seismic capacity, (4) the MOD1 and TRG patterns are almost identical representing a lower seismic capacity than the average. Comparing these results with the nonlinear time history analysis performed by **Akbas et al. (2003)**, it is evident that the WVLP1 pattern results in a seismic capacity that is in good agreement with the results of the nonlinear time history analysis.

For the selected pushover load patterns, Figs. 4a-4f show the normalized ultimate base shear (V_{ult}/W) and the ductility reduction factor ($R\mu$), calculated beyond the collapse prevention level, for the 6-, 9- and 12-story models. The inverse relation between the increase of (V_{ult}/W) ratio and the decrease of ($R\mu$) factor is clear; meanwhile, it reflects the aforementioned effect of pushover load pattern on the seismic capacity. In addition to the collapse (ultimate) stage, the pushover results have been analyzed at three performance levels, namely: operational (drift=D/H=0.25%), life safety (drift=D/H=0.5% and drift=D/H=1%), and collapse prevention (drift=D/H=2%). The results have been listed in Table 2. The resulted minimum, maximum and average responses are consistent with the aforementioned observations in capacity curves in relation to the applied lateral load pattern. It is worth noting that the resulted values for the response reduction factor (R), upon considering the over-strength and redundancy, shall be beyond the values specified in the **ECP-201 (2007).**

Figs. 5a-5c show the inter-story drift ratio (IDR) versus the story level for the 6-, 9- and 12-story models, respectively. The IDR has been calculated for the set of pushover load patterns. For the 6-story model, which represents the low-rise model, the IDR ratio is almost identical for the six patterns with slight differences at the lower and upper floors. However, for the 12-story model, which represents the mid-rise model, there is significant difference in the IDR ratio among different lateral load patterns. In Fig. 5c, it is clear that the WVLP1 and the UNF patterns result in an upper bound for the IDR from the first floor to the sixth floor; meanwhile, they result in a lower bound beyond the sixth floor. On the other hand, the WVLP2 pattern results in a lower bound for the IDR ratio from the first to the

sixth floor; meanwhile, it results in an upper bound beyond the sixth floor. Such differences in the calculated IDR ratio for different pushover load patter are attributed to the difference in the shear load distribution over the building height. This can be effectively visualized in Fig. 6 that shows the normalized pushover load patterns to the UNF pattern for the 12-story model.

5. Summary and Conclusions

This study has analyzed the effect of lateral load pattern on the seismic performance of low-to-mid-rise RC frame buildings. Three building models: 6-, 9- and 12-story have been designed according to the Egyptian codes ECP-201 and ECP-203 and have been subject to pushover load analysis. The lateral load patterns are selected as: uniform (UNF), inverted triangle (TRG), first mode (MOD1), IBC, and weighted-load vector (WLVP1) and (WLVP2). The pushover analysis has been performed for each RC model under the set of six lateral load patterns. SAP2000 program has been used in the analysis and the plastic hinge properties of FEMA 356 have been interfaced. For each model and, in turn, for each lateral load pattern, the capacity curve has been developed and a set of seismic responses have been investigated, namely: base shear, ductility reduction factor, and inter-story drift ratio. The main conclusions can be summarized as follows: (1) the capacity curve is affected by the choice of pushover load pattern, which may under- or over-estimate the building seismic capacity, (2) the UNF pattern represents an upper bound for seismic capacity and a lower bound for ductility reduction factor, (3) the WVLP2 and IBC patterns represent a lower bound for seismic capacity and an upper bound for the ductility reduction factor, (4) the WVLP1 pattern represents an average for both seismic capacity and ductility reduction factor, (5) the MOD1 and TRG patterns are almost identical representing a lower seismic capacity than the average, (6) comparing the analysis results with the nonlinear time history analysis performed by **Akbas et al. (2003)**, it is evident that the WVLP1 pattern results in a seismic capacity that is in good agreement with the results of the nonlinear time history analysis, (7) the IDR ratio is affected by the choice of pushover load pattern due to the difference in the lateral load distribution over the building height, and (8) generally, the weighted-vector load patterns (WVLP1) and (WVLP2) present good upper and lower bounds for most of the global and story seismic demands for mid-rise RC frames.

Table 1. Dimensions, Reinforcement, and Characteristics of Building Models

		6-Story Story number		9-Story Story number			12-Story Story number			
		1,2,3	4,5,6	1,2,3	4,5,6	7,8,9	1,2,3	4,5,6	7,8,9	10,11,12
Beams	Profile (m)	0.25x0.6	0.25x0.6	0.25x0.7	0.25x0.6	0.25x0.6	0.25x0.7	0.25x0.6	0.25x0.6	0.25x0.6
	RFT. (T&B)	4Φ16	4Φ16	5Φ16	4Φ16	4Φ16	5Φ16	4Φ16	4Φ16	4Φ16
	RFT. (%)	0.54%	0.54%	0.57%	0.54%	0.54%	0.57%	0.54%	0.54%	0.54%
Edge Columns	Profile (m)	0.30x0.6	0.30x0.4	0.30x0.8	0.30x0.6	0.30x0.4	0.30x1.0	0.30x0.8	0.30x0.6	0.30x0.4
	RFT.	10Φ16	6Φ16	12Φ16	10Φ16	6Φ16	16Φ16	12Φ16	10Φ16	6Φ16
	RFT. (%)	1.12%	1.01%	1.01%	1.12%	1.01%	1.07%	1.01%	1.12%	1.01%
Inner Columns	Profile (m)	0.30x1.0	0.30x0.8	0.30x1.2	0.30x1.0	0.30x0.8	0.40x1.2	0.30x1.2	0.30x1.0	0.30x0.8
	RFT.	16Φ16	12Φ16	18Φ16	16Φ16	12Φ16	24Φ16	18Φ16	16Φ16	12Φ16
	RFT. (%)	1.07%	1.01%	1.01%	1.07%	1.01%	1.01%	1.01%	1.07%	1.01%
Fundamental Period (Sec.)	SAP2000	0.89		1.17			1.52			
	ECP-201 T= 0.075 H$^{3/4}$	0.68		0.91			1.13			
	ECP-201 T= 0.1 N	0.6		0.9			1.2			

Table 2. Pushover Analysis Results at Three Performance Levels namely: Operational (drift=*D/H*=0.25%), Life Safety (drift=*D/H*=0.5% and drift=*D/H*=1%), and Collapse Prevention (drift=*D/H*=2%) for 6-, 9- and 12-Story Models

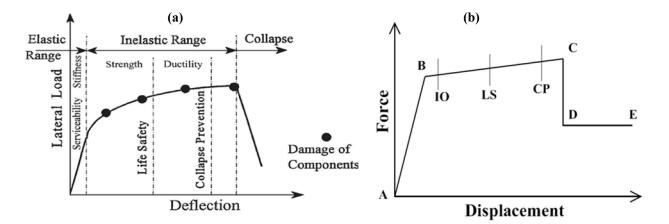|		6A									
		TRG	UNF	MOD1	IBC	WVLP1	WVLP2	MAX	MIN	AVERAGE	STANDARD DEVIATION
D/H = 0.25%	(V/W)%	9.96	11.66	10.08	9.73	10.55	9.53	11.66	9.53	10.25	0.77
	R	1.00	1.00	1.00	1.00	1.00	1.00	1.00	1.00	1.00	0.00
	PEAK (IDR%)	0.34	0.38	0.35	0.34	0.37	0.35	0.38	0.34	0.36	0.02
D/H = 0.5%	(V/W)%	11.60	13.30	11.67	11.41	12.12	11.21	13.30	11.21	11.88	0.76
	R	1.48	1.32	1.00	1.44	1.42	1.49	1.49	1.00	1.36	0.19
	PEAK (IDR%)	0.71	0.77	0.72	0.70	0.75	0.69	0.77	0.69	0.72	0.03
D/H = 1.0%	(V/W)%	12.07	13.89	12.12	11.88	12.59	11.67	13.89	11.67	12.37	0.81
	R	2.96	2.63	1.76	2.88	2.85	2.98	2.98	1.76	2.68	0.47
	PEAK (IDR%)	1.43	1.50	1.44	1.41	1.47	1.40	1.50	1.40	1.44	0.04
D/H = 2.0%	(V/W)%	12.36	14.05	12.38	12.19	12.80	12.00	14.05	12.00	12.63	0.74
	R	5.93	5.26	3.51	5.77	5.69	5.97	5.97	3.51	5.36	0.94
	PEAK (IDR%)	2.86	2.97	2.90	2.77	2.93	2.73	2.97	2.73	2.86	0.09
		9A									
		TRG	UNF	MOD1	IBC	WVLP1	WVLP2	MAX	MIN	AVERAGE	STANDARD DEVIATION
D/H = 0.25%	(V/W)%	7.79	9.84	7.74	7.38	8.46	6.98	9.84	6.98	8.03	1.01
	R	1.00	1.00	1.00	1.00	1.00	1.00	1.00	1.00	1.00	0.00
	PEAK (IDR%)	0.38	0.37	0.39	0.38	0.38	0.39	0.39	0.37	0.38	0.01
D/H = 0.5%	(V/W)%	9.12	10.99	9.04	8.72	9.68	8.33	10.99	8.33	9.31	0.94
	R	1.69	1.58	1.67	1.77	1.84	1.71	1.84	1.58	1.71	0.09
	PEAK (IDR%)	0.76	0.73	0.77	0.78	0.75	0.80	0.80	0.73	0.77	0.02
D/H = 1.0%	(V/W)%	9.55	9.55	9.46	9.18	10.10	8.82	10.10	8.82	9.44	0.43
	R	3.39	3.17	3.34	3.53	3.68	3.42	3.68	3.17	3.42	0.17
	PEAK (IDR%)	1.42	1.41	1.43	1.45	1.40	1.49	1.49	1.40	1.43	0.03
D/H = 2.0%	(V/W)%	9.98	11.86	9.98	9.61	10.49	9.22	11.86	9.22	10.19	0.92
	R	6.78	6.33	6.68	7.07	7.36	6.84	7.36	6.33	6.84	0.35
	PEAK (IDR%)	2.69	2.72	2.70	2.73	2.68	2.74	2.74	2.68	2.71	0.02
		12A									
		TRG	UNF	MOD1	IBC	WVLP1	WVLP2	MAX	MIN	AVERAGE	STANDARD DEVIATION
D/H = 0.25%	(V/W)%	5.93	7.29	5.85	5.50	6.47	5.11	7.29	5.11	6.03	0.77
	R	1.00	1.00	1.00	1.00	1.00	1.00	1.00	1.00	1.00	0.00
	PEAK (IDR%)	0.39	0.40	0.40	0.38	0.42	0.39	0.42	0.38	0.40	0.01
D/H = 0.5%	(V/W)%	7.15	8.97	7.04	6.63	7.69	6.14	8.97	6.14	7.27	0.98
	R	1.88	1.77	1.83	1.59	1.77	1.73	1.88	1.59	1.76	0.10
	PEAK (IDR%)	0.84	0.84	0.85	0.83	0.88	0.83	0.88	0.83	0.84	0.02
D/H = 1.0%	(V/W)%	7.85	9.82	7.76	7.34	8.40	6.84	9.82	6.84	8.00	1.03
	R	3.75	3.55	3.66	3.17	3.54	3.46	3.75	3.17	3.52	0.20
	PEAK (IDR%)	1.53	1.57	1.55	1.54	1.60	1.57	1.60	1.53	1.56	0.03
D/H = 2.0%	(V/W)%	8.21	10.26	8.12	7.71	8.80	7.23	10.26	7.23	8.39	1.06
	R	7.50	7.09	7.32	6.35	7.09	6.93	7.50	6.35	7.05	0.40
	PEAK (IDR%)	2.75	2.94	2.77	2.76	2.92	2.84	2.94	2.75	2.83	0.08

Figure 1. (a) Typical Performance Curve for the Structure, and (b) Typical Plastic Hinge Behaviour (FEMA 356)
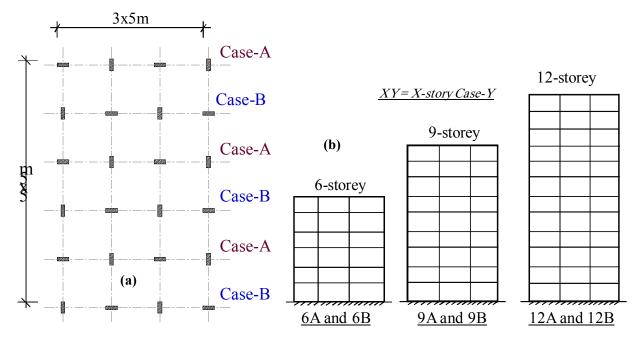

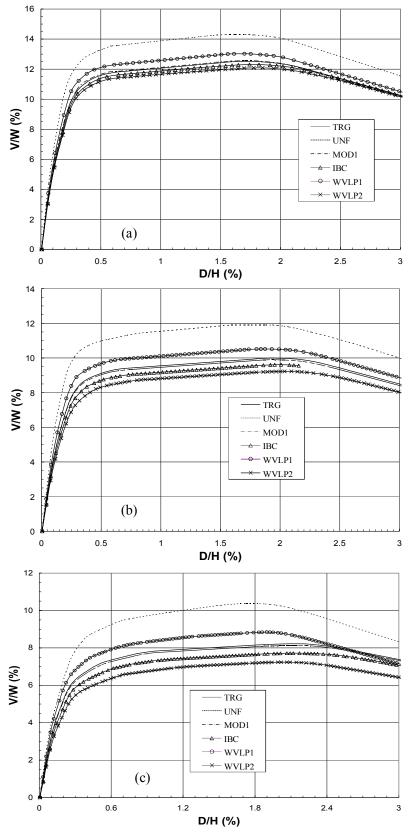**Figure 2. Building Models: (a) Typical Floor Plan, and (b) Typical Elevations**

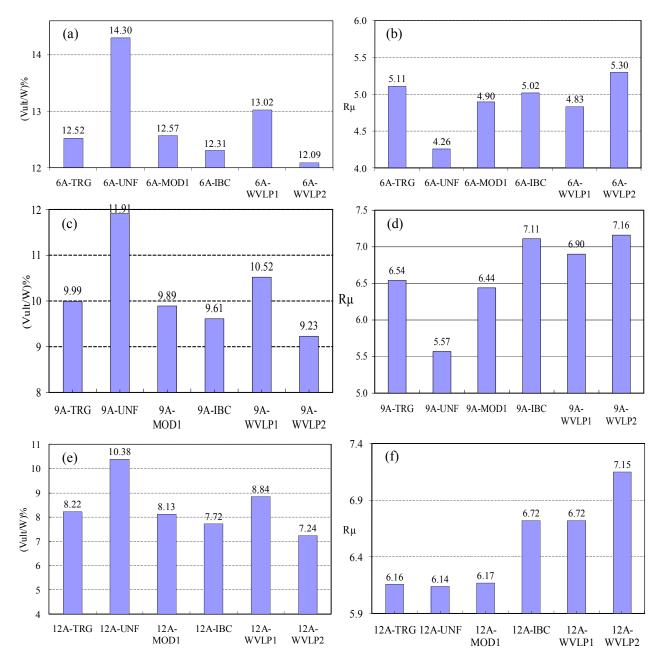**Figure 3. Capacity Curve for: (a) 6-story model, (b) 9-story model, and (c) 12-story model**

Figure 4. Pushover Analysis Results: (a) 6-Story (V$_{ult}$/W) Ratio, (b) 6-Story Rμ Factor, (c) 9-Story (V$_{ult}$/W) Ratio, (d) 9-Story Rμ Factor, (e) 12-Story (V$_{ult}$/W) Ratio, and (f) 12-Story Rμ Factor
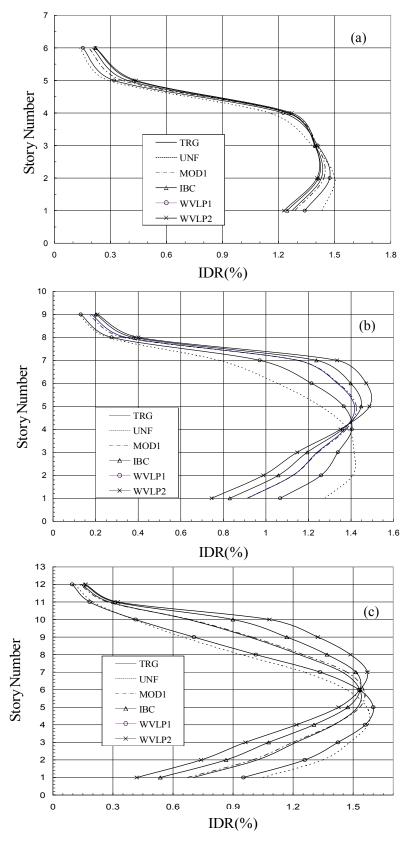
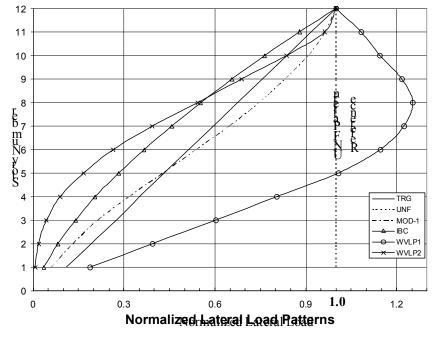**Figure 5. Pushover Analysis Results: (a) 6-Story IDR, (b) 9-Story IDR, and (c) 12-Story IDR**

Figure 6. Normalized Lateral Load Patterns for 12-Story Model

Corresponding author
Mohammed Hassanien Serror
Assistant Professor, Dept. of Structural Engineering,
Faculty of Engineering, Cairo University, Egypt
mhassanien@cosmos-eng.com

References
1. Akbas B, Shen J, Kara FI, Tugsal UM (2003). Seismic Behavior and Pushover Analysis in Steel Frames. The 5th National Conference on Earthquake Engineering; AT-053, Istanbul, Turkey.
2. ATC 40 (1996). Seismic evaluation and retrofit of existing concrete buildings. Redwood City (CA): Applied Technology Council.
3. Chopra AK, Goel, RK (2002). A Model Pushover Analysis Procedure for Estimating Seismic Demands for Buildings. Earthquake Engineering and Structural Dynamics; 31: 561-582.
4. CSI (2010). Computers & Structures, Inc. www.csiberkely.com.
5. ECP-201 (1993). Egyptian Code for Calculating Loads and Forces in Structural Work and Masonry, National Research Center for Housing and Building, Giza, Egypt.
6. ECP-201 (2007). Egyptian Code for Calculating Loads and Forces in Structural Work and Masonry, National Research Center for Housing and Building, Giza, Egypt.
7. ECP-203 (2007). Egyptian Code for Design and Construction of Reinforced Concrete Structures, National Research Center for Housing and Building, Giza, Egypt.
8. El-Esnawy, NA (2007). Advanced Multi-Mode Pushover Method for Estimating Peak Seismic Drifts of Mid-Rise Steel Buildings. Scientific Bulletin, Faculty of Engineering, Ain Shams University; 42(3): 265-287.
9. FEMA-273 (1997). Prestandard and Commentary for the Seismic Rehabilitation of Buildings, Federal Emergency Management Agency, Washington, DC, U.S.A.
10. FEMA-356 (2000). Prestandard and Commentary for the Seismic Rehabilitation of Buildings, Federal Emergency Management Agency, Washington, DC, U.S.A.
11. Ghobarah A (2001). Performance Based Design in Earthquake Engineering: State of Development. Engineering Structures; 23: 878-884.
12. IBC (2003). International Building Code, International Code Council, Virginia, U.S.A.
13. Inel M, Tjhin T, Aschheim MA (2003). The Significance of Lateral Load Pattern in Pushover Analysis. The 5th National Conference on Earthquake Engineering; AE-009, Istanbul, Turkey.
14. Jianguo N, Kai Q, Yan X (2006). Push-Over Analysis of the Seismic Behavior of a Concrete-Filled Rectangular Tubular Frame Structure. Tsinghua Science and Technology; 11(1): 124-130.
15. SEAOC Vision 2000 (1995). Performance Based Seismic Engineering of Buildings, vols. I and II: Conceptual framework. Sacramento (CA): Structural Engineers Association of California.

12/12/2011